A room-temperature study of the kinetics and energetics for the protonation of ethane

G. I. MACKAY, H. I. SCHIFF, AND D. K. BOHME

Department of Chemistry and Centre for Research in Experimental Space Science, York University, Downsview, Ont., Canada M3J 1P3

Received November 3, 1980

This paper was presented at a Special Symposium "The Structure and Thermochemistry of Gaseous Ions", held in honour of Dr. F. P. Lossing, of the National Research Council of Canada, during the Second Canadian Conference on the Gas Phase Chemistry of Ions, Trent University, June 5–8, 1980, and is dedicated to him on the occasion of his 65th birthday

G. I. MACKAY, H. I. SCHIFF, and D. K. BOHME. Can. J. Chem. **59**, 1771 (1981).

The flowing afterglow and selected-ion flow tube (SIFT) techniques have been applied in room-temperature measurements of the kinetics for proton-transfer reactions of ethane with HeH^+, H_3^+, N_2H^+, CH_5^+, N_2OH^+, and HCO^+. The fragmentation of $C_2H_7^+$ was followed over a range in excess energy of 100 kcal mol^{-1}. Equilibrium constants were measured at low excess energies for the proton-transfer reactions with HCO^+ and N_2OH^+. The latter provided values for the proton affinity of ethane and $\Delta H_f^0(C_2H_7^+)$ and, indirectly, values for the proton affinity of ethylene and $\Delta H_f^0(C_2H_5^+)$. Additional measurements of the kinetics of the reactions of C_2H_6 with H^+ itself, O^+, OH^+, and H_2O^+ provided insight into the competition between proton-transfer and other reaction channels and the fragmentation associated with the $C_2H_6^+$ ion.

G. I. MACKAY, H. I. SCHIFF et D. K. BOHME. Can. J. Chem. **59**, 1771 (1981).

Opérant à la température ambiante, on a utilisé les techniques de la lueur d'écoulement et de tube à écoulement d'ions sélectionnés (TEIS) pour mesurer la cinétique des réactions de transfert de proton de l'éthane avec HeH^+, H_3^+, N_2H^+, CH_5^+, N_2OH^+ et HCO^+. On a contrôlé la fragmentation de $C_2H_7^+$ sur une large étendue d'énergie en excès de 100 kcal mol^{-1}. On a mesuré les constantes d'équilibre en utilisant de faibles énergies en excès pour les réactions de transfert du proton avec HCO^+ et N_2OH^+. Ces dernières permettent de déterminer les valeurs de l'affinité de l'éthane pour le proton et le $\Delta H_f^0(C_2H_7^+)$ et, indirectement, les valeurs de l'affinité de l'éthylène pour le proton ainsi que la $\Delta H_f^0(C_2H_5^+)$. Des mesures additionnelles des cinétiques des réactions du $C_2H_6^+$ avec H^+ lui-même, O^+, OH^+ et H_2O^+ fournissent de nouvelles connaissances quant à la compétition entre le transfert de proton et d'autres voies de réaction et de la fragmentation associée avec l'ion $C_2H_6^+$.

[Traduit par le journal]

Introduction

The low stability of $C_2H_7^+$ against dissociation into $C_2H_5^+$ and H_2 has presented a special challenge to the determination of the tendency for ethane to gain a proton. Here we report a systematic investigation of the kinetics and energetics for the protonation of ethane by reactions of the type:

$$[1] \quad AH^+ + C_2H_6 \rightarrow [C_2H_7^+]^* + A \longrightarrow C_2H_5^+ + H_2$$

We adopted the approach which we have recently applied to studies of the dissociative protonation of other molecules such as nitromethane (1), formic and acetic acid (2), and several formate and acetate esters (3). The method involves the preparation of a variety of acids, AH^+, by prereaction in a Flowing Afterglow or Selected Ion Flow Tube apparatus, which are then invoked systematically in proton-transfer reactions of type [1]. The concomitant variation in excess energy allowed the nature and extent of the fragmentation of $C_2H_7^+$ to be monitored in a controlled fashion as a function of the degree of its chemical activation by AH^+. Furthermore, several relatively mild acids were identified for which the fragmentation was minimal. Their reactions with ethane permitted the involvement of $C_2H_7^+$ in an equilibrium state and consequently the determination of the relative proton affinity of ethane from equilibrium constant measurements (4). An extension of these studies to radical cations and H^+ itself introduced still other competing channels together with the fragmentation associated with the $C_2H_6^+$ ion.

Experimental

The experiments were carried out using both the Flowing Afterglow, FA, and Selected Ion Flow Tube, SIFT, techniques for which details of construction and methods of operation have been described elsewhere (4, 5). The equilibrium measurements were made with the conventional flowing afterglow using H_2 as the carrier gas. N_2OH^+ and HCO^+ ions were produced from H_3^+ according to the following rapid reactions:

$$[2] \quad H_3^+ + N_2O \rightarrow N_2OH^+ + H_2$$

$$[3] \quad H_3^+ + CO \rightarrow HCO^+ + H_2$$

The H_3^+ itself was established as usual by the rapid reaction of H_2 with H_2^+ produced by electron impact on the carrier gas in the region of the electron gun. The ethane was added sufficiently downstream of the ion production region to ensure that reactions [2] and [3] had gone to completion and that the N_2OH^+ and HCO^+ ions had thermalized to the ambient temperature of 298 ± 2 K.

Except for the reaction of ethane with CH_5^+ which was

0008-4042/81/121771-08$01.00/0

followed in a H_2 carrier in the flowing afterglow mode, the kinetic measurements were carried out with the apparatus in the SIFT configuration. Helium was employed as the carrier gas in the reaction region while both H_2 and He were used in the source region at total pressures of ca. 0.5 Torr. CH_5^+ was produced in the manner of reactions [2] and [3]. H_3^+, HCO^+, and N_2H^+ were produced in the SIFT source as in the FA mode. The OH_x^+ ions were produced from water vapour introduced into a SIFT source containing a weak He plasma.

The purities of the gases have been given previously (6) except that for ethane which was 99.9% (Matheson Research Grade).

Results

The data analysis associated with the determination of rate constants and equilibrium constants has been described in detail elsewhere together with the various sources of error (4, 5).

H^+, HeH^+, H_3^+

With the SIFT quadrupole tuned to H_3^+ both H^+ and HeH^+ were observed to be produced in the reaction tube containing helium buffer at pressures in the range 0.357 to 0.50 Torr. The translational energy acquired by the H_3^+ apparently was sufficient to cause some collisional dissociation:

[4*a*] $H_3^+ + He \rightarrow H^+ + H_2 + He$

and to overcome the endothermicity of the proton-transfer reaction:

[4*b*] $H_3^+ + He \rightarrow HeH^+ + H_2$

Figure 1 shows the response of these ions to the addition of ethane into the reaction region sufficiently downstream to allow for their thermalization. All three are rapidly replaced by the ions $C_2H_3^+$, $C_2H_4^+$, and $C_2H_5^+$ in a distribution with respect to the three individual reactant ions which is not readily discernable from the data. The $C_2H_3^+$ is known to react further with ethane to produce $C_2H_5^+$ (7). There was no evidence for the formation of $C_2H_7^+$ (< 1%).

$C_2H_5^+$ is the only one of the three observed product ions which may be formed exothermically by the reaction of ethane with thermalized H_3^+, so that we may write:

[5] $H_3^+ + C_2H_6 \rightarrow C_2H_5^+ + 2H_2$

The formation of both $C_2H_3^+$ and $C_2H_5^+$ is exothermic for the reaction with HeH^+:

[6] $HeH^+ + C_2H_6 \rightarrow C_2H_5^+ + H_2 + He$
$\rightarrow C_2H_3^+ + 2H_2 + He$

Because of the small initial signal of HeH^+ only a small fraction of the observed $C_2H_3^+$ can be attributed to reaction [6]. The $C_2H_4^+$ and most of the $C_2H_3^+$ must, by elimination, come from the free protons:

[7] $H^+ + C_2H_6 \rightarrow C_2H_4^+ + H_2 + H$
$\rightarrow C_2H_3^+ + 2H_2$

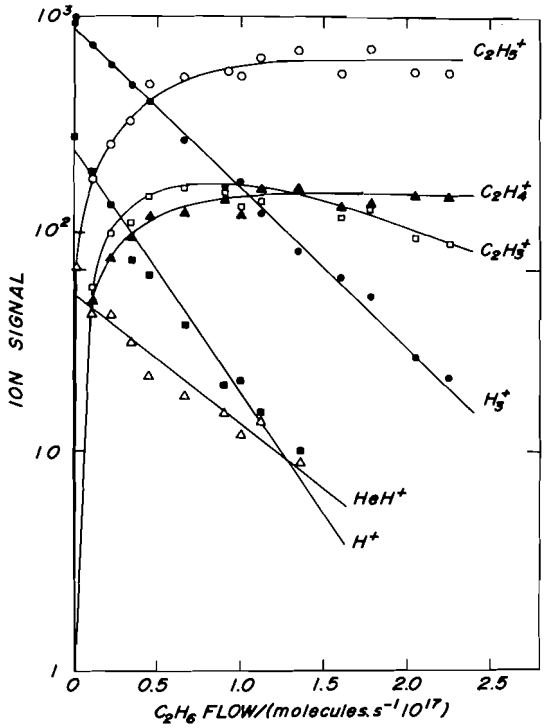

FIG. 1. The variation in ion signals detected upon the addition of C_2H_6 into the reaction region with the SIFT quadrupole tuned to H_3^+ and He Buffer gas in the flow tube. $T = 297$ K, $L = 46$ cm, $P = 0.366$ Torr, and $\bar{v} = 8.5 \times 10^3$ cm s^{-1}.

N_2H^+, CH_5^+

The reaction of N_2H^+ with ethane was investigated in the SIFT mode with H_2 as carrier gas. Figure 2 shows a representative observation of changes in ion signals. The decay of the N_2H^+ is masked in this case by the rise in $C_2H_5^+$ at $m/e = 29$ as is evident from the concomitant rise in the $m/e = 30$ isotope of $C_2H_5^+$. A fit to the rise in the $m/e = 31$ signal provided a rate constant of 1.3×10^{-9} cm^3 molecule^{-1} s^{-1} with an uncertainty of 35%. 87% of the reactive collisions apparently lead to $C_2H_5^+$:

[8] $N_2H^+ + C_2H_6 \rightarrow C_2H_5^+ + H_2 + N_2$
$\rightarrow C_2H_7^+ + N_2$

The association reaction:

[9] $C_2H_5^+ + H_2 \rightarrow C_2H_7^+$

which may ensue in the H_2 buffer is too slow to alter significantly the $C_2H_5^+/C_2H_7^+$ branching ratio under our operating conditions. Experiments in which $C_2H_5^+$ was injected into H_2 buffer at typical

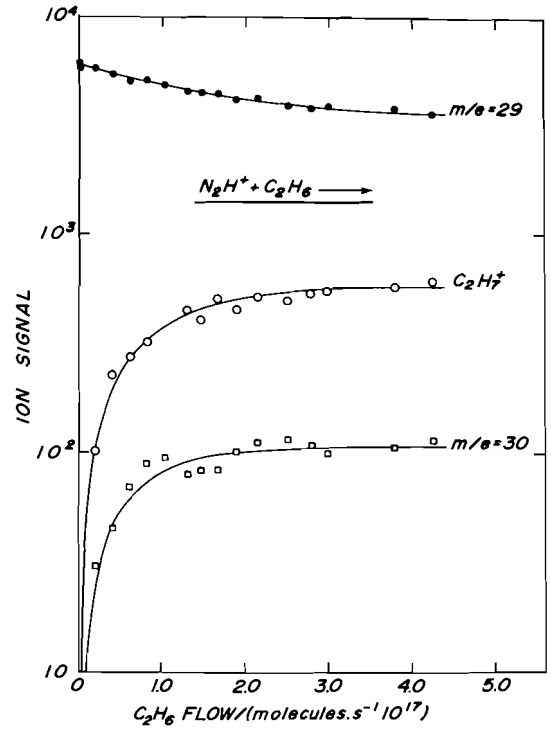

FIG. 2. The variation in ion signals recorded upon the addition of C_2H_6 into the reaction region with the SIFT quadrupole tuned to N_2H^+ and H_2 buffer gas in the flow tube. T = 300 K, L = 46 cm, P = 0.347 Torr, and $\bar{v}$ = 7.6 × 10^3 cm s^{-1}.

operating pressures failed to reveal any formation of $C_2H_7^+$. This observation is consistent with the results obtained by Hiraoka and Kebarle (8) who observed reaction [9] to be second order overall at H_2 pressures down to 2.4 Torr and to have a rate constant of only about 1 × 10^{-14} cm^3 molecule^{-1} s^{-1} at 298 K.

The protonation of ethane by CH_5^+ was investigated in a H_2 buffered flowing afterglow at total pressures from 0.420 to 0.51 Torr. The decays of CH_5^+ were observed to be linear and indicated rapid reaction with k = 1.5 × 10^{-9} cm^3 molecule^{-1} s^{-1} and an estimated uncertainty of ± 25%. Both $C_2H_7^+$ and $C_2H_5^+$ were observed as product ions in the ratio of 5.5 ± 1.0 to 1 under these operating conditions:

[10] $CH_5^+ + C_2H_6 \rightarrow C_2H_7^+ + CH_4$
$\rightarrow C_2H_5^+ + H_2 + CH_4$

The linearity of the observed CH_5^+ decays persisted for at least three orders of magnitude over a range of methane flows from 4.27 × 10^{17} up to 1.9 × 10^{19} molecules s^{-1} which is indicative of a slow reverse reaction and a high equilibrium constant.

N_2OH^+

Rapid protonation of ethane was also observed to occur in H_2 buffer in which N_2OH^+ was initially a dominant ion. Other exothermic channels which lead to the formation of a m/e = 31 ion are conceivable but these involve considerable bond redisposition and could be ruled out on the basis of the observed m/e = 32 ion which had the correct isotopic abundance for $C_2H_7^+$. Some formation of an ion at m/e = 29($C_2H_5^+$) was again apparent but in much smaller relative amounts, about 5%:

[11] $N_2OH^+ + C_2H_6 \rightarrow C_2H_7^+ + N_2O$
$\rightarrow C_2H_5^+ + H_2 + N_2O$

Sufficient curvature was introduced into the N_2OH^+ decays at flows of N_2O from 5.25 × 10^{17} to 1.87 × 10^{19} molecules s^{-1} to allow for the analysis of the kinetics for the reverse reaction and the establishment of equilibrium for the reaction:

[11a] $N_2OH^+ + C_2H_6 = C_2H_7^+ + N_2O$

as demonstrated in Fig. 3 and Fig. 4, respectively. The total pressure was in the range from 0.300 to 0.424 Torr.

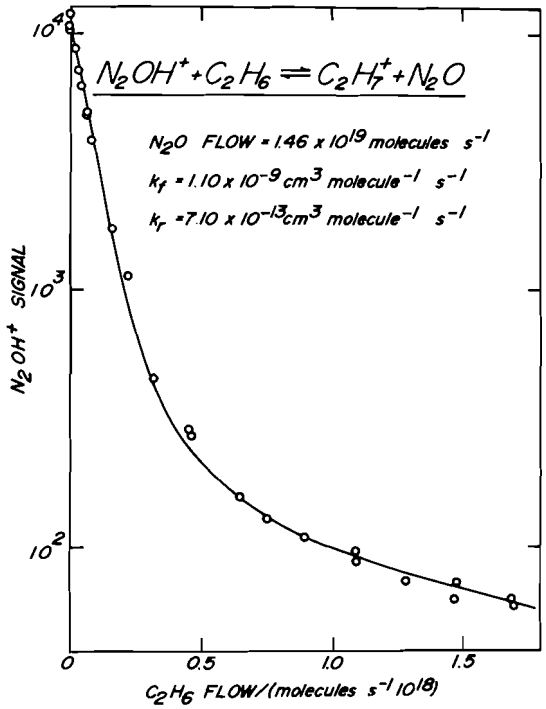

FIG. 3. The variation of the N_2OH^+ signal observed as a function of the flow of ethane at a fixed flow of N_2O in the flowing afterglow mode. T = 296 K, L = 85 cm, P = 0.405 Torr, and $\bar{v}$ = 8.3 × 10^3 cm s^{-1}. The open circles are experimental and the curve is calculated using the values indicated for k_f, k_r, and the flow of N_2O.

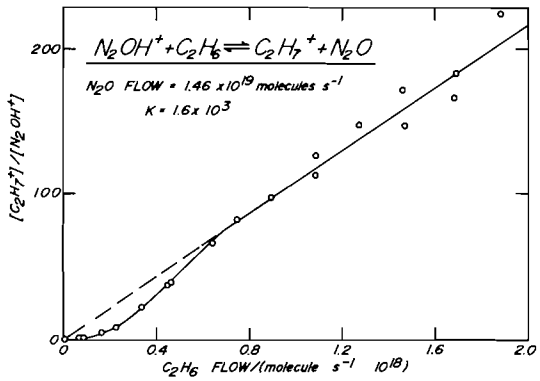

FIG. 4. The observed variation in the ion concentration ratio $[C_2H_7^+]/[N_2OH^+]$ (corrected for mass discrimination) as a function of ethane addition showing the approach to and attainment of equilibrium at a fixed flow of N_2O in the flowing afterglow. The best straight line through the open circles at high ethane flows yields the indicated value for the equilibrium constant.

Thirteen runs provided a value for the forward rate constant of $(1.1 \pm 0.2) \times 10^{-9}$ cm^3 molecule^{-1} s^{-1}. In nine of these runs the curvature in the decays of N_2OH^+ provided a reverse rate constant of $(6.9 \pm 2.1) \times 10^{-13}$ cm^3 molecule^{-1} s^{-1} and a ratio of rate constants of $(1.5 \pm 0.45) \times 10^3$. The measured ratio of equilibrium concentrations provided a value for K of $(1.5 \pm 0.3) \times 10^3$ which is identical to the rate constant ratio.

HCO^+

The proton-transfer reaction of HCO^+ with ethane was expected to have a small equilibrium constant on the basis of the N_2OH^+ results and the known proton affinities of N_2O and CO (9). Indeed, strong curvature was observed in the decays of HCO^+ at all flows of CO which ranged from 1.53×10^{18} to 9.9×10^{19} molecules s^{-1} and at total pressures from 0.331 to 0.420 Torr. Equilibrium appeared to be established in the flowing afterglow already at small additions of ethane. The curvature in the HCO^+ decay was fitted to provide a ratio of rate constants of 10.8 ± 3.2. Because of the early establishment of equilibrium the fitting procedure could not yield unique values for the individual rate constants. The analysis of the equilibrium ratio plots yielded a value for K of 11.9 ± 4.0 which combines with the measured ratio of rate constants to provide a true value for the thermodynamic equilibrium constant of 11.3 ± 2.4. This value is in excellent accord with the ratio of equilibrium constants $(1.5 \pm 0.3) \times 10^3/(1.4 \pm 0.2) \times 10^2 = 11 \pm 4$ derived from the equilibrium constant measurements for reactions [11*a*] and [12] (10):

[12] $N_2OH^+ + CO = HCO^+ + N_2O$

The SIFT measurements performed with H_2 buffer gas at pressures between 0.283 and 0.451 Torr and in the absence of CO in the reaction region, provided a rate constant for the protonation of ethane by HCO^+ of $(1.2 \pm 0.2) \times 10^{-10}$ cm^3 molecule^{-1} s^{-1}. There was no evidence for any formation of $C_2H_5^+$.

OH_x^+

The reactions of O^+, OH^+, and H_2O^+ with ethane were investigated in the SIFT mode in helium buffer gas at pressures in the range 0.298 to 0.359 Torr. All three ions reacted rapidly with the added ethane and at least two product ions were apparent in each case. With O^+ the apparent reaction was the following:

[13] $O^+ + C_2H_6 \rightarrow C_2H_4^+ + (H_2O)$
$\rightarrow C_2H_5^+ + (OH)$

The observed branching ratio $C_2H_4^+/C_2H_5^+$ was 7/3. The proton affinity of O is close to that of N_2 (9) so that the proton transfer from OH^+ to ethane is quite exothermic. But so are many other reaction channels in this instance. Indeed, the product spectrum observed in this case was quite elaborate:

[14*a*] $OH^+ + C_2H_6 \rightarrow C_2H_4^+ + (H_2 + OH)$

[14*b*] $\rightarrow C_2H_5^+ + (H_2 + O)$

[14*c*] $\rightarrow H_3O^+ + C_2H_4$

[14*d*] $\rightarrow C_2H_6^+ + OH$

[14*e*] $\rightarrow C_2H_7^+ + O$

The observed branching ratio was a:b:c:d:e = 65:20:10:3:2. Proton transfer appears to be completely swamped by other reaction channels in the case of H_2O^+ for which it is still exothermic but now only slightly so. The observed product spectrum was the following:

[15*a*] $H_2O^+ + C_2H_6 \rightarrow H_3O^+ + C_2H_5$

[15*b*] $\rightarrow C_2H_4^+ + H_2 + H_2O$

[15*c*] $\rightarrow C_2H_6^+ + H_2O$

[15*d*] $\rightarrow C_2H_5^+ + H + H_2O$

Evidently H-atom transfer predominates almost exclusively as the branching ratio a:b:c:d was estimated to be 83:12:4:1.

Discussion

The measurements reported in this study yield both rate and equilibrium data for the protonation of ethane. The latter provides the basis for a determination of the proton affinity of ethane as

will be discussed in a later section. The former provides insight into the efficiency of protonation, the stability of the resulting $C_2H_7^+$ against further dissociation, and the degree to which proton transfer competes with other reaction channels when these become viable options, as is the case with radical ions.

Kinetics of Protonation

Table 1 summarizes the rate constants determined in this study along with the observed product ion distributions. Except for the reaction of HCO^+ which proceeds at only about 10% efficiency, all of the reactions in Table 1 proceed within 25% of the collision rate calculated from the Langevin (11) or Average-Quadrupole-Orientation, AQO, theories (12, 13).

The free protons were observed to react most rapidly. Their reaction proceeded at 80% of the AQO rate. The observed $C_2H_4^+$ and $C_2H_3^+$ product ions may be envisaged to arise from what is formally a dissociative hydride ion transfer:

$$[16]\quad H^+ + C_2H_6 \rightarrow [C_2H_7^+]^* \rightarrow \begin{cases} [C_2H_5^+]^* + H_2 \\ \rightarrow C_2H_4^+ + H \\ \rightarrow C_2H_3^+ + H_2 \end{cases}$$

and/or by dissociative charge transfer:

$$[17]\quad H^+ + C_2H_6 \rightarrow [C_2H_6^+]^* + H \begin{cases} \rightarrow C_2H_5^+ + H \\ \rightarrow C_2H_4^+ + H_2 \end{cases}$$

However, the formation of $C_2H_3^+$ by dissociative charge transfer may be ruled out since it is endothermic.

It is interesting to compare the reaction with protons to that with O^+ ions since H and O atoms have essentially identical ionization potentials. The reaction with O^+ seems more efficient with the measured rate constant being 25% larger than the calculated collision rate constant. $C_2H_4^+$ is a major product but $C_2H_3^+$ is not observed even though the overall exothermicities of the H^+ and O^+ reactions are very similar. $C_2H_5^+$ appears as a product ion instead. The higher stability of $C_2H_5^+$ in this case may arise from a larger amount of the excess energy appearing in the neutral OH in the analogue of reaction [16].

An inspection of the product distributions in Table 1 for the reactions of the even-electron acids AH^+ = HeH^+, H_3^+, N_2H^+, CH_5^+, N_2OH^+, and HCO^+, reveals the trend expected on the basis of the dissociative proton-transfer mechanism expressed in eq. [1]. The most energetic product ions $C_2H_3^+$ and $C_2H_5^+$ are associated with the strongest acid

TABLE 1. Summary of rate constants and product distributions for reactions with ethane measured in this study at 298 ± 2 K

Reactant ion	Product ions	Product distribution	Rate constant[a]
H^+	$C_2H_4^+$ $C_2H_3^+$ $(C_2H_5^+)$		3.9 ± 0.8
O^+	$C_2H_4^+$ $C_2H_5^+$	0.7 0.3	1.9 ± 0.4
OH^+	$C_2H_4^+$ $C_2H_5^+$ H_3O^+ $C_2H_6^+$ $C_2H_7^+$	0.65 0.20 0.10 0.03 0.02	1.6 ± 0.3
H_2O^+	H_3O^+ $C_2H_4^+$ $C_2H_6^+$ $C_2H_5^+$	0.83 0.12 0.04 0.01	1.6 ± 0.3
HeH^+	$C_2H_5^+$ $C_2H_3^+$		2.1 ± 0.4
H_3^+	$C_2H_5^+$	1.00	2.4 ± 0.5
N_2H^+	$C_2H_5^+$ $C_2H_7^+$	0.87 0.13	1.3 ± 0.5
CH_5^+	$C_2H_7^+$ $C_2H_5^+$	0.85 0.15	1.5 ± 0.3
N_2OH^+	$C_2H_7^+$ $(C_2H_5^+)$	0.95 0.05	1.1 ± 0.2
HCO^+	$C_2H_7^+$	1.00	0.12 ± 0.02

[a] Rate constant for the total loss of the reactant ion along with the estimated accuracy in units of 10^{-9} cm^3 molecule^{-1} s^{-1}.

HeH^+ for which the excess energy is largest, while the least energetic product ion $C_2H_7^+$ is associated predominantly with the weakest acid in this series, HCO^+, for which the excess energy is smallest.

The trend in the product distribution with reaction exothermicity observed in this study for the protonation of C_2H_6 is shown in the form of a bargraph in Fig. 5. Clearly the fraction of $C_2H_7^+$ ions which have sufficient energy to decompose, and do so under the experimental conditions, increases dramatically when the reaction exothermicity exceeds the 13.0 kcal mol^{-1} required for the dissociation as is indicated in the potential energy diagram shown in the insert in Fig. 5. The observed efficiency of dissociative proton transfer will depend on the total energy initially deposited in the $C_2H_7^+$ product, the dependence of the rate constant of the fragmentation on this internal energy, and the degree to which the internal energy is moderated by collisions with the buffer gas molecules. Since the time between collisions with the buffer gas molecules is ca. 1 μs, fragmentations

TABLE 2. Product distributions observed for various degrees of excitation of ions in reactions with ethane

Reaction	Product ions[a]	Product distribution: Tandem-ICR[b] Excited	Tandem-ICR[b] Relaxed	FA[c]
$N_2H^+ + C_2D_6/C_2H_6$	$C_2D_6H^+$	0.00	0.09	0.13
	$C_2D_5^+ + C_2D_4H^+$	1.00	0.91	0.87
$CD_5^+/CH_5^+ + C_2H_6$	$C_2H_6D^+$	0.26	0.58	0.85
	$C_2H_5^+ + C_2H_4D^+$	0.74	0.42	0.15
$N_2OD^+/N_2OH^+ + C_2H_6$	$C_2H_6D^+$		0.89	0.95
	$C_2H_5^+$, $C_2H_4D^+$		0.11	0.05
$DCO^+/HCO^+ + C_2D_6/C_2H_6$	$C_2D_7^+$		0.84	1.00
	$C_2D_5^+$		0.16	0.00

[a]Only the deuterated product ions observed in the tandem-ICR experiments are indicated. The FA experiments were carried out only with undeuterated reactants.

[b]Reactions proceeded at average ion translational energies of 0.1 eV and typical pressures of 10^{-6} Torr. The average number of ion–neutral collisions of an ion prior to reaction was varied between 0 and 10 collisions by increasing the pressure in the ion source.

[c]Product distributions measured in the flowing afterglow or SIFT mode at 298 ± 2 K.

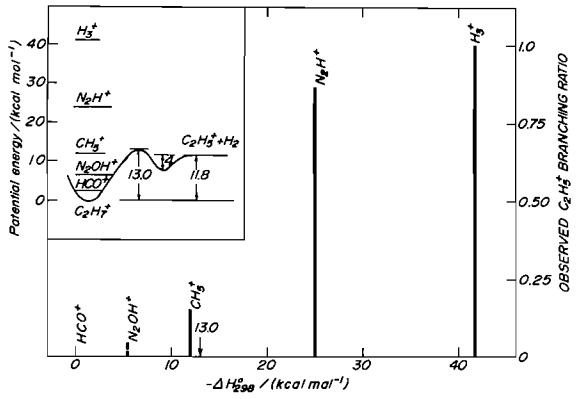

FIG. 5. The observed trend in the extent of dissociative proton transfer to C_2H_6 with reaction exothermicity. The exothermicities have been calculated from the proton affinities determined previously in this laboratory (9) and that of C_2H_6 derived in the text. The potential energy diagram is based on rate and equilibrium measurements for the association of $C_2H_5^+$ and H_2 as a function of temperature carried out by Hiraoka and Kebarle (8).

which require more time than this may be discriminated against and so obscure the initial product distribution in that they may appear as stabilized $C_2H_7^+$ product ions.

It is interesting to compare, as is done in Table 2, the product distributions observed at the relatively high pressures of the FA/SIFT experiments with those obtained previously at the much lower pressures, viz. 10^{-6} Torr, of tandem-ICR experiments (14). In the latter experiments the product distributions were found to be quite sensitive to the excitation of the reactant ion AH^+, shifting towards decreased dissociation of the $C_2H_7^+$ with an increase in the average number of ion–neutral collisions experienced by AH^+ prior to reaction. The product distributions obtained in the FA/SIFT experiments, in which the reactant ions experience a sufficient number of ion–neutral collisions to be thermalized to the buffer gas temperature, are consistent with the trend established at the low pressures in that they show a still further shift towards $C_2H_7^+$ formation. The further shift is expected since there still is a spread in internal energies of several tenths of an eV associated with the "relaxed" AH^+ ions in the tandem-ICR experiments. For example, for the proton-transfer reaction with HCO^+ for which the flowing afterglow measurements show no dissociation, and indeed the dissociation is clearly endothermic, the tandem-ICR experiments show that 16% of the reaction produces $C_2H_5^+$. Dissociative proton-transfer is also endothermic for N_2OH^+ but in this case the energetics are somewhat unique in that several other exothermic routes are possible for the observed formation of the ion at $m/e = 29$:

$$[18a]\quad N_2OH^+ + C_2H_6 \rightarrow C_2H_5^+ + H_2O + N_2$$

$$[18b]\quad \rightarrow N_2H^+ + C_2H_5OH/(C_2H_4 + H_2O)$$

Channels [18*a*] and [18*b*] are exothermic by 69 and 36/(26) kcal mol^{-1}, respectively. Channel [18*a*] seems more probable on mechanistic grounds since it can be viewed to proceed by hydride transfer to N_2OH^+ followed by the dissociation of the resulting neutral species into stable N_2 and H_2O.

Proton Affinity of Ethane

The results of the pertinent equilibrium constant

measurements are shown in Table 3. They provide a best estimate of the true value of the equilibrium constant for the protonation of ethane by HCO^+ of 11.2 ± 2.1:

[19] $HCO^+ + C_2H_6 = C_2H_7^+ + CO$

This result is very useful for the determination of the proton affinity of ethane since the proton affinity of CO is well established. The equilibrium constant corresponds to a standard free energy change at 298 K for reaction [19] of -1.43 ± 0.11 kcal mol^{-1}. A standard entropy change of $+2.3 \pm 2.2$ cal mol^{-1} K^{-1} may be estimated from the absolute entropies for HCO^+, $C_2H_7^+$, and CO, of 48.04 ± 0.2 (15), 54.9 (16), 58 ± 3, and 47.21 (17) cal mol^{-1} K^{-1}. The entropy of $C_2H_7^+$ was estimated from a comparison with the entropies of the isoelectronic species CH_3NH_2 and CH_3OH and ethane itself (16). The standard free energy and entropy changes can be combined to provide a value for the standard enthalpy change of -0.74 ± 0.77 kcal mol^{-1}, or a difference in the proton affinities of C_2H_6 and CO, $\Delta PA(C_2H_6, CO) = 0.7 \pm 0.8$ kcal mol^{-1}. With a value for PA(CO) of 141.4 ± 0.4 kcal mol^{-1} as in ref. 9, the value for $PA(C_2H_6)$ becomes 142.1 ± 1.2 kcal mol^{-1}. This result is consistent with the limiting values $136 < PA(C_2H_6) < 159$ kcal mol^{-1} which we obtained previously from bracketing measurements (18), but it exceeds the value of 127.0 ± 1.0 kcal mol^{-1} obtained on the basis of mass-spectrometer ion-source measurements (19) of the proton-transfer reaction:

[20] $CH_5^+ + C_2H_6 = C_2H_7^+ + CH_4$

This discrepancy has been discussed previously (18). *Ab initio* molecular orbital calculations (20) of the geometry and energy of $C_2H_7^+$ have led to a theoretical value for $PA(C_2H_6) = 140.1$ kcal mol^{-1} (not corrected for zero point vibrations) which compares very favourably with our experimental value. Accepted heats of formation for ethane and the proton (16, 17) lead to a heat of formation for $C_2H_7^+$ of 204.8 ± 1.3 kcal mol^{-1}.

TABLE 3. Summary of equilibrium constants measured at 298 ± 2 K for proton-transfer reactions of the type $XH^+ + Y \rightleftharpoons YH^+ + X$. The preferred direction of proton transfer is towards the top of the table

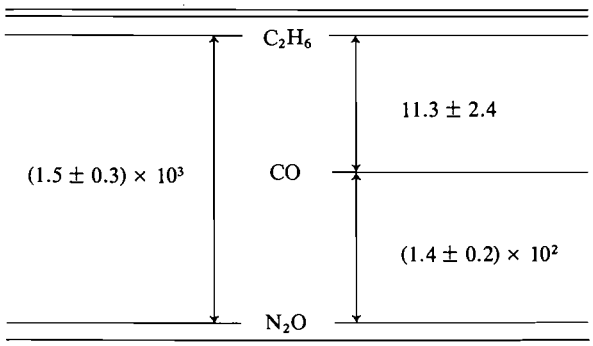

Proton Affinity of Ethylene

Having established a value for the proton affinity of ethane, we may take advantage of previous measurements of the equilibrium constant for the association reaction [9] to derive a value for the proton affinity of ethylene. Equilibrium [9] has been investigated by Hiraoka and Kebarle (8) between 358 and 473 K in a high-pressure ion-source mass spectrometer. The corresponding van't Hoff plot provided a value for the standard enthalpy change for reaction [9] of -11.8 ± 0.4 kcal mol^{-1}. $PA(C_2H_4)$ is related to this enthalpy change and $PA(C_2H_6)$ by the equation:

[21] $PA(C_2H_4) = PA(C_2H_6) + \Delta H_f^0(C_2H_4) - \Delta H_f^0(C_2H_6) - \Delta H_9^0$

The accepted values for the heats of formation of ethylene and ethane (16) lead to a value for $PA(C_2H_4) = 163.0 \pm 1.7$ kcal mol^{-1}. Also the heat of formation of $C_2H_7^+$ determined above leads to a heat of formation for $C_2H_5^+$ of 216.6 ± 1.7 kcal mol^{-1}.

The heat of formation of $C_2H_5^+$ has recently received renewed attention. Previous values have been based exclusively on non-equilibrium studies of the appearance of this ion by dissociative ionization and by the ionization of the ethyl radical and have led to a higher value of 220.5 kcal mol^{-1} (21) (here the electron is treated as a conventional element (17)). The shortcomings of these two methods have been described recently by Baer in connection with a report of results obtained by him in a photoionization and photoion-photoelectron coincidence (PIPECO) study of the appearance of $C_2H_5^+$ from C_2H_5I (22). The onset of $C_2H_5^+$ in the I atom loss process:

[22] $h\nu + C_2H_5I \rightarrow C_2H_5^+ + I + e$

was measured in delayed coincidence with zero energy electrons. The kinetic energy release was also measured and found to be zero at the dissociation onset. Baer has derived from these observations a room-temperature heat of formation for $C_2H_5^+$ of 216.8 ± 1.0 kcal mol^{-1} (or 215.3 ± 1.0 kcal mol^{-1} with the stationary electron convention (21)) which is in excellent agreement with the value obtained in our study.

Acknowledgement

We thank the Natural Sciences and Engineering Research Council of Canada for financial support.

1. G. I. MACKAY and D. K. BOHME. Int. J. Mass Spectrom. Ion Phys. **26**, 327 (1978).
2. G. I. MACKAY, A. C. HOPKINSON, and D. K. BOHME. J. Am. Chem. Soc. **100**, 7460 (1978).
3. A. C. HOPKINSON, G. I. MACKAY, and D. K. BOHME. Can. J. Chem. **57**, 2996 (1979).
4. D. K. BOHME, R. S. HEMSWORTH, H. W. RUNDLE, and H. I. SCHIFF. J. Chem. Phys. **58**, 3504 (1973).
5. G. I. MACKAY, G. D. VLACHOS, D. K. BOHME, and H. I. SCHIFF. Int. J. Mass Spectrom. Ion Phys. **36**, 259 (1980).
6. G. I. MACKAY, L. D. BETOWSKI, J. D. PAYZANT, H. I. SCHIFF, and D. K. BOHME. J. Phys. Chem. **80**, 2919 (1976).
7. L. W. SIECK and S. G. LIAS. J. Phys. Chem. Ref. Data, **5**, 1123 (1976).
8. K. HIRAOKA and P. KEBARLE. J. Am. Chem. Soc. **98**, 6119 (1976).
9. D. K. BOHME, G. I. MACKAY, and H. I. SCHIFF. J. Chem. Phys. **73**, 4976 (1980).
10. R. S. HEMSWORTH, H. W. RUNDLE, D. K. BOHME, H. I. SCHIFF, D. B. DUNKIN, and F. C. FEHSENFELD. J. Chem. Phys. **59**, 61 (1973).
11. G. GIOUMOUSIS and D. P. STEVENSON. J. Chem. Phys. **29**, 294 (1958).
12. T. SU and M. T. BOWERS. Int. J. Mass Spectrom. Ion Phys. **17**, 309 (1975).
13. T. SU and M. T. BOWERS. Int. J. Mass Spectrom. Ion Phys. **21**, 417 (1976).
14. R. D. SMITH and J. H. FUTRELL. Int. J. Mass Spectrom. Ion Phys. **20**, 347 (1976).
15. P. J. BRUNA. Ap. L. **16**, 107 (1975).
16. D. D. WAGMAN, W. H. EVANS, V. B. PARKER, I. HALOW, S. M. BAILY, and R. H. SCHUMM. Natl. Bur. Stand. Tech. Note 207–3 (1968).
17. JANAF Thermochemical Tables, 2nd ed., Natl. Bur. Stand. Ref. Data Ser. 37 (1971).
18. D. K. BOHME, P. FENNELLY, R. S. HEMSWORTH, and H. I. SCHIFF. J. Am. Chem. Soc. **95**, 7512 (1973).
19. S. L. CHONG and J. L. FRANKLIN. J. Am. Chem. Soc. **94**, 6347 (1972).
20. W. A. LATHAN, W. J. HEHRE, and J. A. POPLE. J. Am. Chem. Soc. **93**, 808 (1971).
21. H. M. ROSENSTOCK, K. DRAXL, B. W. STEINER, and J. T. HERRON. J. Phys. Chem. Ref. Data Suppl. **1**, 6 (1977).
22. T. BAER. J. Am. Chem. Soc. **102**, 2482 (1980).